Gas separation performance of 6FDA-based polyimides with different chemical structures

Wulin Qiu [a], Liren Xu [a], Chien-Chiang Chen [a], Donald R. Paul [b], William J. Koros [a], *

[a] School of Chemical and Biomolecular Engineering, Georgia Institute of Technology, 778 Atlantic Drive, Atlanta, GA 30332-0100, USA
[b] Department of Chemical Engineering and Texas Materials Institute, The University of Texas at Austin, Austin, TX 78712, USA

ABSTRACT

This work reports the gas separation performance of several 6FDA-based polyimides with different chemical structures, to correlate chemical structure with gas transport properties with a special focus on CO_2 and CH_4 transport and plasticization stability of the polyimides membranes relevant to natural gas purification. The consideration of the other gases (He, O_2 and N_2) provided additional insights regarding effects of backbone structure on detailed penetrant properties. The polyimides studied include 6FDA-DAM, 6FDA-mPDA, 6FDA-DABA, 6FDA-DAM:DABA (3:2), 6FDA-DAM:mPDA (3:2) and 6FDA-mPDA:DABA (3:2). Both pure and binary gas permeation were investigated. The packing density, which is tunable by adjusting monomer type and composition of the various samples, correlated with transport permeability and selectivity. The separation performance of the polyimides for various gas pairs were also plotted for comparison to the upper bound curves, and it was found that this family of materials shows attractive performance. The CO_2 plasticization responses for the un-cross-linked polyimides showed good plasticization resistance to CO_2/CH_4 mixed gas with 10% CO_2; however, only the cross-linked polyimides showed good plasticization resistance under aggressive gas feed conditions (CO_2/CH_4 mixed gas with 50% CO_2 or pure CO_2). For future work, asymmetric hollow fibers and carbon molecular sieve membranes based on the most attractive members of the family will be considered.

© 2013 Elsevier Ltd. All rights reserved.

1. Introduction

Natural gas is an important global energy source, and high concentrations of CO_2 must be removed prior to pipeline transportation and use. In some cases, CO_2 level can be as high as 70% at pressures up to 5000 psia [1–3]. The currently dominant technology for CO_2 removal from natural gas relies upon amine absorption, which can present environmental concerns as well as capital and maintenance costs of the large absorption units. Membrane separation offers a potentially more energy efficient technology with smaller capital cost and physical footprint, as well as minimal environmental concerns [1,3,4]. Commercially available polymeric membranes (polysulfone, cellulose acetate, etc.) are limited by their permeability and selectivity performance [5,6]. Polyimides, especially the 6FDA-based polyimides membranes offer excellent intrinsic CO_2/CH_4 separation properties, thermal, chemical and mechanical stability [3,7–13] and are processable using current commercial fabrication processes. Despite these advantages, unless stabilized by crosslinking, plasticization under aggressive feed conditions (high pressure, high CO_2 content) causes loss of selectivity and hence separation efficiency [3,7,8,10,13–18]. Several approaches including cross-linking have been used to address plasticization of polymers [7,14,19,20]. In our group, we have pursued ester cross-linking of 6FDA-DAM:DABA membranes using a diol [7,10,21,22], and recently decarboxylation-induced thermal cross-linking [8]. Decarboxylation-induced thermal cross-linking occurs at elevated temperatures (~ 15 °C above the glass transition temperature) for 6FDA-DAM:DABA (2:1) polyimide membranes; however, such high temperatures may result in the densification of transition layers and porous substructures of asymmetric hollow fibers. To avoid such densification effects, thermal cross-linking of 6FDA-DAM:DABA (3:2) copolymer below the polymer's glass transition temperature (~ 387 °C by DSC) was shown to be possible [17]. This previous work showed that both the thermal treatment temperature and time influence the degree of cross-linking. Nevertheless, this earlier study showed that essentially complete thermal cross-linking of 6FDA-DAM:DABA (3:2) dense film membrane can be carried out even at a temperature as low as 330 °C [17]. Perhaps surprisingly, decarboxylation-induced thermal cross-linking causes a marked increase in

* Corresponding author. Tel.: +1 404 385 2845.
 E-mail address: wjk@chbe.gatech.edu (W.J. Koros).
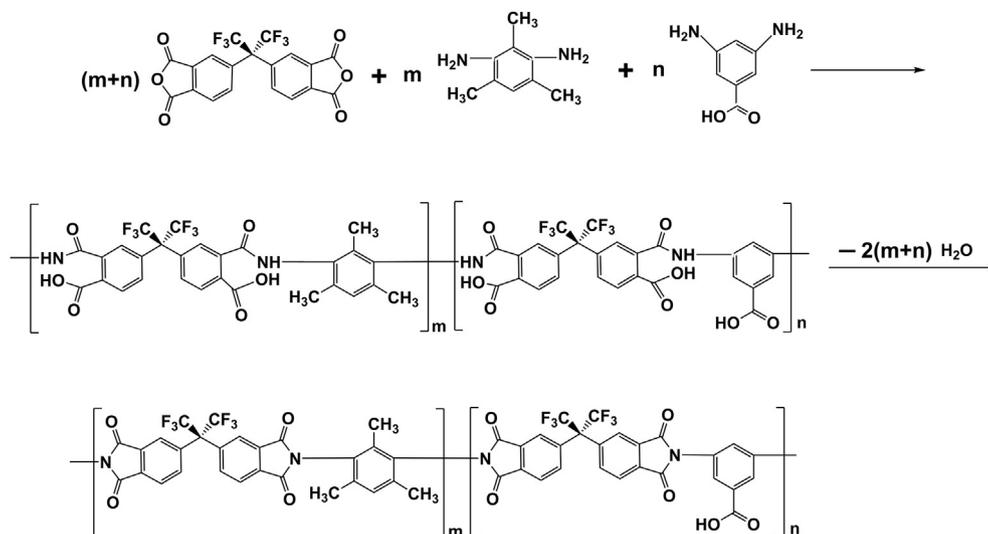
Scheme 1. Synthesis of 6FDA-DAM:DABA polyimide.

permeability for gases, e.g., He, O_2, N_2, CH_4, and CO_2, and a slight decrease in CO_2/CH_4 selectivity, presumably due to reduced segmental packing. The selectivity of the cross-linked membrane is maintained even under very aggressive CO_2 operating conditions beyond those without cross-linking. Plasticization resistance was demonstrated even up to 700 psia for pure CO_2 gas or at 1000 psia for 50/50 CO_2/CH_4 mixed gas [17]. The sub-T_g thermal crosslinking approach was subsequently extended to 6FDA-DAM:DABA (3:2) asymmetric hollow fiber membranes without damaging the delicate skin and porous substructure or high selectivities of defect free fibers [23].

The gas separation performance is inherently determined by the polymer's chemical structure and correlates with the physical structure of the polymer and corresponding properties [24–30]. Adjusting diamine and dianhydride allows flexible tuning of chemical structure, transport properties, and stability within this diverse family. In this article, we expand and further explore the correlation of chemical structures of a broader array of 6FDA polymers and their corresponding gas transport properties, especially with regard to permeability-selectivity-plasticization relationships. In this paper, five new polyimides are considered for comparison to the previously considered 6FDA-DAM:DABA material. Correlation of chemical structures of 6FDA polymers and their corresponding gas transport properties, using the systematic set of polyimide considered here provides a useful framework for optimum selection of materials of aggressive feed gas separations.

2. Background and theory

Permeability and selectivity provide measures of intrinsic productivity and separation capability of a membrane, respectively for a selected A vs. B pair. Permeability (P_A) in units of Barrers (eq. (1)) is equal to the transmembrane partial pressure (or fugacity) difference (Δp_A or Δf_A) and membrane thickness (l) normalized penetrant diffusive flux (n_A), as shown in eqs. (2a) and (2b). For high feed pressures, it is more appropriate to describe the permeation driving force in terms of a fugacity difference (Δf_i) rather than a partial pressure difference in eq. (2) to calculate component permeabilities. In this work, fugacity coefficients of CO_2 and CH_4 in binary mixtures were calculated from the virial equation of state [31] using the pure-component second virial coefficients [32] and the second virial coefficient for the binary mixture [31].

$$1 \text{ Barrer}[=]10^{-10}\frac{\text{cm}^3(\text{STP})\cdot\text{cm}}{\text{cm}^2\cdot\text{s}\cdot\text{cm Hg}} \tag{1}$$

$$P_i = \frac{(n_i)\cdot l}{(\Delta p_i)} \tag{2a}$$

or,

$$P_i = \frac{(n_i)\cdot l}{(\Delta f_i)} \tag{2b}$$

The ideal selectivity between penetrants A and B, defined as the ratio of their permeabilities (eq. (3)), equals the mixed-gas "separation factor" (eq. (4)) when the downstream pressure is negligible, as it is in the current study.

$$\alpha_{AB} = \frac{P_A}{P_B} \tag{3}$$

$$\alpha_{AB} = \frac{(y_A/y_B)}{(x_A/x_B)} \tag{4}$$

where x_i and y_i are the mole fraction of component i in the feed side and permeate, respectively.

3. Experimental

3.1. Materials

Monomers (4,4'-hexafluoroisopropylidene) diphthalic anhydride (6FDA), 2,4,6-trimethyl-1,3-diaminobenzene (DAM), m-Phenylenediamine (mPDA), and 3,5-diaminobenzoic acid (DABA) were purchased from Aldrich. Monomers were purified through sublimation or recrystallization, and stored separately under high vacuum before synthesis. Solvents and reagents, 1-methyl-2-pyrrolidinone (NMP), acetic anhydride (AcAn), and beta picoline were dried with molecular sieves before use.

3.2. Polymer synthesis

Polyimides were synthesized via the well-known condensation of the dianhydride with diamine as shown in Scheme 1 for 6FDA-
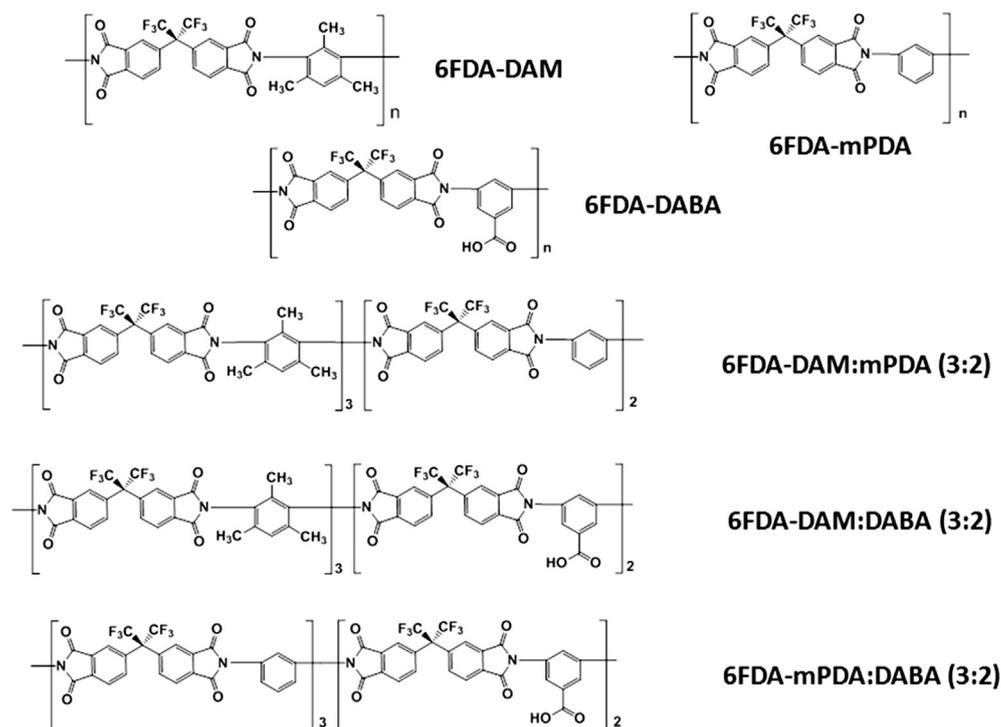
Scheme 2. Polyimides chemical structure.

DAM:DABA, as an illustrative example for all polyimides. The first step produces a high molecular weight polyamic acid (PAA) at low temperature (~ 5 °C) followed by the second step for ring-closing imidization. In the first step, stoichiometric amounts of monomers were agitated and reacted in a 20 wt% NMP solution under N_2 purge for 24 h to produce the PAA solution. Chemical imidization was achieved in the presence of beta picoline and acetic anhydride at ambient temperature for 24 h under N_2 purge, and the resulting polyimide (PI) was precipitated and washed with methanol and dried at 210 °C under vacuum for 24 h. The FTIR and TGA results of the resulting polyimide show essentially complete imidization.

3.3. Membrane formation

Dense film was cast on a Teflon coated glass plate from a THF solution inside a glove bag with controlled atmosphere to achieve slow evaporation of solvents. A casting knife with a 12 mil clearance was used for film casting, and after evaporation of THF solvent, the membrane was removed from the plate, and dried at 180 °C for 24 h under vacuum. The typical film thickness is about 60 microns. TGA results of membranes showed no detectable residual solvent.

3.4. Polymer characterization

The molecular weight, glass transition temperature, and thermal stability of the new polymers considered here for transport studies were provided elsewhere [16], and thermal degradation behaviors were correlated with their chemical structures [16]. The esterification and cross-linking degree of 6FDA-DAM:DABA (3:2) and the PDMC-PI (polyimide with a propyl monoester moiety attached to the carboxylic acid groups in 6FDA-DAM:DABA) was tracked via a straightforward thermogravimetric analysis (TGA) method to complement gas permeation testing of plasticization response for cross-linked samples [16,17]. Wide-angle X-ray diffraction (WAXD) was also measured on a PAnalytical X'pert Pro diffractometer operating with a Cu Kα radiation at a wavelength of

1.54 Å, in a 2θ range of 5–45° to consider segmental packing and to verify the lack of crystallinity.

3.5. Membrane permeation test

Dried membranes were used for gas permeation tests following approaches like those reported earlier for 6FDA-DAM:DABA (3:2) membranes [17]. After masking with impermeable aluminum tape and epoxy applied at the interface of tape and the membrane, the mounted samples were evacuated completely and steady-state gas permeabilities were determined at 35 °C.

Pure gas (He, O_2, N_2, CH_4, and CO_2) permeation measurements were made for all polymers while mixed gas (CO_2/CH_4 mixtures with 10% CO_2 and 50% CO_2, respectively) permeation measurements were made for selected polymers, with 2–3 replicates for pure gas measurements, and 4–5 replicates for mixed gas measurements using a Agilent Technologies 6890N gas chromatograph (GC). Replicate film samples (at least two and generally three separate samples for each membrane composition) were found to vary by less than 10% for permeability, and essentially negligibly for selectivity. In our experiments, membranes were exposed to the feed gas longer than 2 h (in some cases about one day). For each test, permeability was calculated from the time that was longer than 10 times of time lag, and repeated tests for several times by pulling vacuum at the downstream. For membrane plasticization tests, we feed CO_2 upstream and meanwhile pull downstream vacuum, start test only after waiting more than 10 times of time lag, and ensue the slope remains unchanged. We also repeat tests several times; then go to next feed pressure while keep downstream in vacuum and wait to get steady state before test, and so on for next feed pressure. It took about one week to complete the plasticization test for a sample to ensure we are studying steady state. It may be that at the highest pressure, some minor on-going creep may occur over days and weeks; however, we already see meaningfully different plasticization behavior for different samples.

Table 1
Characteristics of polyimides.

Polyimide	Mw	PDI	T_g (°C)
6FDA-DAM	514,000	4.1	395
6FDA-mPDA	198,000	2.3	315
6FDA-DABA	15,100	1.9	363
6FDA-DAM:DABA (3:2)	278,000	3.5	387
6FDA-DAM:mPDA (3:2)	258,000	2.5	373
6FDA-mPDA:DABA (3:2)	208,000	7.2	328

4. Results and discussion

4.1. Characterization of 6FDA-based polyimides with related chemical structures

The 6FDA-based polyimides considered here (Scheme 2) were chosen to better understand the connection between polyimide chemical structures and gas permeability, selectivity, crosslinking properties, and plasticization responses. These polyimides with high molecular weight and narrow molecular weight distributions were synthesized and characterized in terms of molecular weight, glass transition, and degradation behavior in our earlier paper [16]. The characteristics of these samples are given in Table 1. Through comparing the plasticization resistance of cross-linked 6FDA-DAM:DABA (3:2) membrane and PDMC-PI membrane to CO_2 with the membranes' thermal degradation behavior, it was found that the TGA method can be used to evaluate crosslinking of DABA-based polyimide membranes without CO_2 permeation tests [16]. To avoid crosslinking, all membranes were dried below the glass transition temperature, i.e., at 180 °C for 24 h under vacuum, and were cooled to room temperature before testing. Under such conditions all of the membranes remained un-crosslinked, as the membranes were easily dissolved at room temperature in solvents such as THF or NMP, and the CO_2 permeation tests also confirmed the lack of crosslinking of the membranes, which will be discussed later. As noted in the introduction, unlike our earlier work [17], which focused on only 6FDA-DAM:DABA (3:2) samples for sub-T_g crosslinking, this work focuses on transport and separation properties of un-crosslinked samples with chemical structures shown in Scheme 2.

Wide-angle X-ray diffraction results in Fig. 1 show that all the polyimides membranes are totally amorphous with broad peaks. The average interchain distances (d-spacing) values were calculated by Bragg's law ($d = \lambda/2\sin\theta$) using the maximum 2θ values of the broad peaks and the 1.54 Å wavelength of the Cu Kα x-ray source. Although d-spacing does not give true interchain distances, changes of d-spacing are indicators of changes in packing density of polymer chains, which affect the ability of small molecules to diffuse through the glassy matrix. The polyimides membranes exhibit d-spacings in the order of 6FDA-DAM (6.8 Å) > 6FDA-DAM:mPDA (6.4 Å) > 6FDA-mPDA (6.0 Å) > 6FDA-DAM:DABA (5.6 Å) > 6FDA-mPDA:DABA (5.2 Å) > 6FDA-DABA (5.1 Å), indicating an increased chain packing from 6FDA-DAM to 6FDA-DABA.

4.2. Gas permeation behaviors in polymers with related chemical structures

Permeabilities of the various polyimides vary significantly, but all of the un-crosslinked membranes showed strong plasticization responses at characteristic CO_2 feed pressures. While the CO_2 permeability of 6FDA-DAM is high, it shows the most extreme plasticization response, and even after aging at room temperature for 7 months strong plasticization response remains (Fig. 2a), so *physical aging does not provide stabilization against aggressive CO_2*
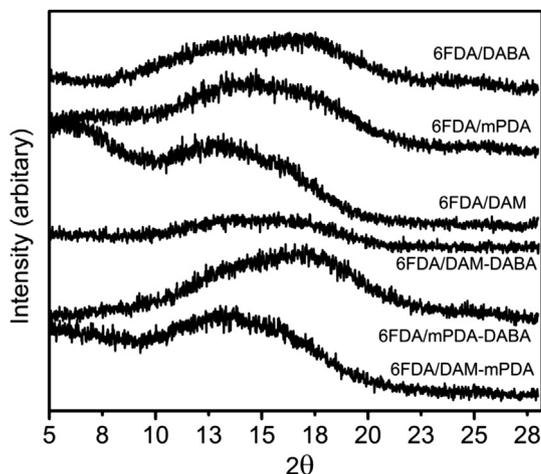
Fig. 1. WAXD scans of polyimide membranes.

feeds. The CO_2 permeability is much higher than reported by Wind [33]. We suspect that the very high Mw and high PDI in Table 1 may be a factor in explaining the differences.

The CO_2 permeability for 6FDA-mPDA (Fig. 2b) is much lower than those in 6FDA-DAM membrane under comparable feed pressures. Despite the difference in absolute permeability level, 6FDA-mPDA shows a minimum permeability of about 20 Barrers at 200 to 300 psia, so plasticization is still clearly apparent. Moreover, after maintaining the membrane at a CO_2 pressure of 820 psia for 20 h, the CO_2 permeability during depressurization tests was found to show a long term conditioning effect. During the depressurization experiments, typically 1 h, was needed before the rate of pressure rise in the downstream receiver volume became constant.

The CO_2 permeability of the 6FDA-DABA (Fig. 2c) membrane was even lower than in 6FDA-mPDA; however, a plasticization response was still found at about 450 psia. The onset of plasticization was higher than for either 6FDA-DAM or 6FDA-mPDA membrane, and this may reflect stabilization by hydrogen bonds among −COOH groups in 6FDA-DABA.

The CO_2 permeability for 6FDA-DAM:DABA (3:2) (studied earlier [16,17]) is shown in Fig. 3a for comparison. For the feed pressures studied, the CO_2 permeability is about 100−250 Barrers, considerably higher than 6FDA-DABA, but much lower than 6FDA-DAM; thereby showing the tunable nature of this polyimide family. As with the other samples, a characteristic plasticization pressure was also seen for 6FDA-DAM:DABA (3:2), and upon dwelling at the highest testing pressure (700 psia of pure CO_2), the permeability increased significantly. The CO_2 permeability in 6FDA-DAM:mPDA (3:2) (Fig. 3b) lies in the range of 200−400 Barrers and show a plasticization response at 200 to 300 psia. As with the other un-crosslinked samples, exposure to the highest CO_2 feed pressure of 700 psia for 20 h cause the permeability to increase dramatically and remain high as feed pressure decreased during depressurization measurements. Finally, consistent with the other 6FDA-based family membranes, 6FDA-mPDA:DABA (3:2) (Fig. 3c) showed a noticeable plasticization response near 300 psia, even though the absolute value of the unplasticized sample (∼10 Barrers) was much lower than the DAM-containing samples.

The CO_2 permeability in polymers with different chemical structures, summarized in Fig. 4, make it obvious that DAM-based polymers (Fig. 4a) have much higher permeabilities than the polyimides band on the other diamines (Fig. 4b). It is also clear that both mPDA and DABA moieties decrease the CO_2 permeability, Table 2 provides a useful summary of CO_2 permeabilities measured at
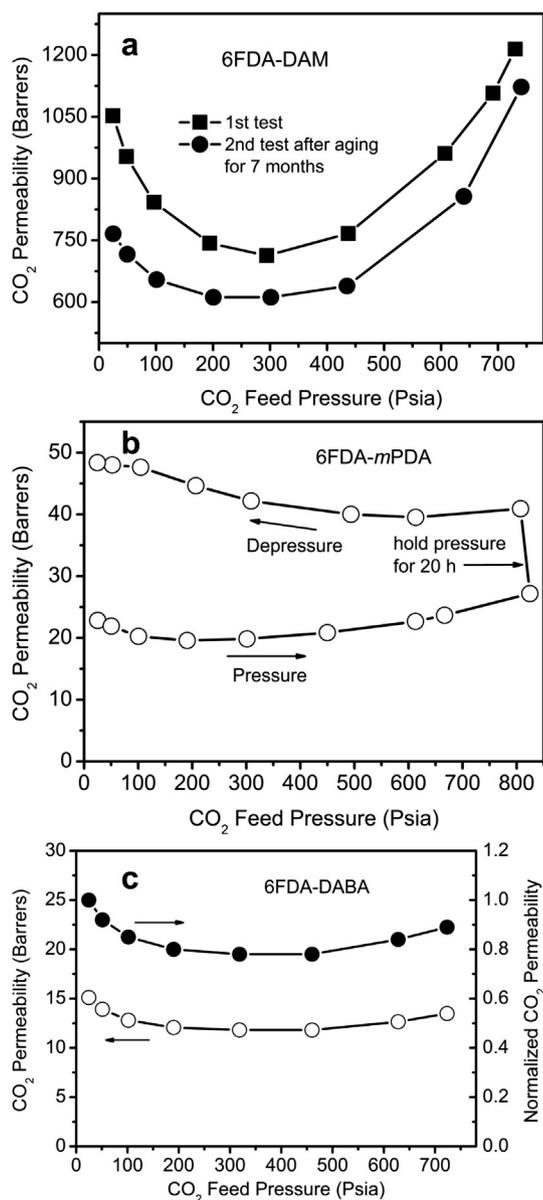
Fig. 2. Pure gas CO_2 permeability of (a) 6FDA-DAM, (b) 6FDA-mPDA, and (c) 6FDA-DABA membranes as a function of feed pressure at 35 °C.

Fig. 3. Pure gas CO_2 permeability of (a) 6FDA-DAM:DABA (3:2), (b) 6FDA-DAM:mPDA (3:2), and (c) 6FDA-mPDA:DABA (3:2) polyimide membrane as a function of feed pressure at 35 °C.

100 psia, while permselectivities are compared in Table 3 for the full range of gas pairs studied. The results were repeated 2–3 times, and standard derivations are less than 0.5% for all gases. These results show clearly the significant impact of structural modification on gas permeability and selectivity. For example, the introduction of three −CH₃ groups onto the diamine moiety of 6FDA-mPDA, i.e., replacing mPDA with DAM to form 6FDA-DAM, induces a 6.6-fold (He) to 117-fold (CH₄) increase in permeability, while a 1.8-fold (O₂/N₂) to 19.7-fold (He/CH₄) decrease in selectivity. Similar trends were found when a single −CH₃ group was introduced [25]. On the other hand, the introduction of a −COOH group in the diamine moiety of 6FDA-mPDA, i.e., replace mPDA with DABA to form 6FDA-DABA, results in 1.5-fold (He) to 2.0-fold (CH₄) decrease in permeability, with less than 1.2-fold increase or no change in selectivity to different gas pairs, as can be seen in Table 3. As one might expect, the 6FDA-DABA (with 5.1 Å d-spacing) has a higher interchain packing density than 6FDA-mPDA (6.0 Å d-spacing), which has lower interchain interactions due to the lack of hydrogen bonds.

In all cases, for a given gas at the same feed pressure, the polyimides showed permeabilities in the following order: 6FDA-DAM ≫ 6FDA-DAM:mPDA (3:2) > 6FDA-DAM:DABA (3:2) ≫ 6FDA-mPDA > 6FDA-DABA > 6FDA-mPDA:DABA (3:2). The co-polymer permeabilities of 6FDA-DAM:DABA (3:2) and 6FDA-DAM:mPDA (3:2) are in the range of the corresponding values of homopolymers, i.e., 6FDA-DAM and 6FDA-DABA, as well as 6FDA-DAM and 6FDA-mPDA. The copolymer permeability of 6FDA-mPDA:DABA (3:2) is smaller than for the non-DABA polymers, indicating that both mPDA and DABA moieties reduce permeability.

The permselectivities in Table 3 for each gas pair tend to show the expected trend for the lowest permeability members, with [6FDA-mPDA:DABA (3:2) and 6FDA-DABA] showing the highest selectivity for any of the gas pairs, while the highest permeability
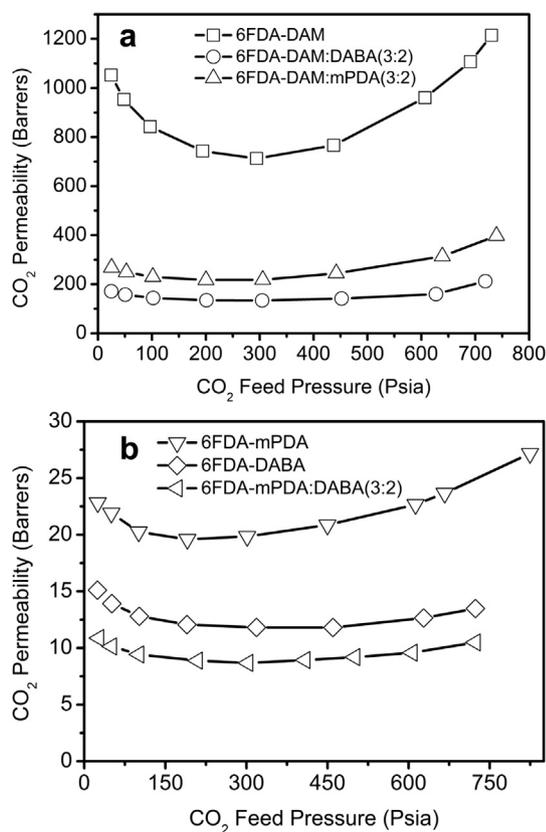
Fig. 4. Pure gas CO_2 permeability of polyimide membranes with different chemical structure as a function of feed pressure at 35 °C.

members [6FDA-DAM and 6FDA-DAM:mPDA (3:2)] showed the lowest selectivity for any of the gas pairs.

It should be especially noted that among the above polyimides, 6FDA-mPDA, 6FDA-DABA, and their copolyimide 6FDA-mPDA:-DABA show high CO_2/CH_4 selectivity. The permeabilities are higher than the commercial polyimide, Matrimid®, which showed a CO_2 permeability of 5–10 Barrers, with a CO_2/CH_4 selectivity about 35 [34,35]. The gas permeation performance of the copolyimides of 6FDA-mPDA:DABA can be tailored by adjusting the monomer ratio during synthesis. Most important, however, is the fact that this sub-family of copolyimides can also be cross-linked through the −COOH group, similar to 6FDA-DAM:DABA copolymer. This makes the 6FDA-mPDA:DABA an especially important polyimide with potential applications in natural gas separation, since it has the potential to be stabilized by either the ester or decarboxylation-based crosslinking demonstrated earlier for 6FDA-DAM:DABA. To pursue this idea, we used the thermal decarboxylation route, since it is simple and avoids using a potentially hydrolyzable ester linkage. The results were dramatically satisfying, with the CO_2 permeability rising from ∼9 Barrer to ∼48 Barrer after the 6FDA-mPDA:DABA (3:2) membrane was thermally treated at 370 °C for 1 h, while the

Table 2
Pure gas permeability of polyimides membranes at 100 psia and 35 °C (Barrers).

Polyimides	He	O_2	N_2	CH_4	CO_2
6FDA-DAM	533.21	191.53	54.99	46.81	842.41
6FDA-mPDA	80.46	5.39	0.87	0.35	20.25
6FDA-DABA	53.24	3.14	0.51	0.20	12.80
6FDA-DAM:DABA (3:2)	195.91	31.99	7.04	4.19	143.95
6FDA-DAM:mPDA (3:2)	238.93	52.08	12.46	7.94	230.21
6FDA-mPDA:DABA (3:2)	42.74	2.51	0.40	0.16	9.14

Table 3
Pure gas selectivity of polyimides membranes at 100 psia and 35 °C.

Polyimides	He/CH_4	He/N_2	O_2/N_2	O_2/CH_4	CO_2/CH_4	CO_2/N_2	N_2/CH_4
6FDA-DAM	11.4	9.7	3.5	4.1	18.0	15.3	1.2
6FDA-mPDA	229.4	92.3	6.2	15.4	57.7	23.2	2.5
6FDA-DABA	258.9	104.1	6.1	15.3	62.2	25.0	2.5
6FDA-DAM:DABA (3:2)	46.8	27.8	4.5	7.6	34.4	20.4	1.7
6FDA-DAM:mPDA (3:2)	30.1	19.2	4.2	6.6	29.0	18.5	1.6
6FDA-mPDA:DABA (3:2)	267.1	106.9	6.3	15.7	57.1	22.9	2.5

CO_2/CH_4 selectivity was maintained at about 53. A similar trend for CO_2 permeability to increase with only slight decreases in CO_2/CH_4 selectivity was also observed in thermally crosslinked 6FDA-DAM:DABA polymers. This trend was believed to be due to extra free volume created during crosslinking [8,17]. We believe a similar explanation applied to other DABA-based polyimides. A similar trend was also observed for a ester bond crosslinked 6FDA-mPDA:DABA (9:1) membrane, where the CO_2 permeability increased from 6.5 Barrer to 9.5 Barrer while the CO_2/CH_4 selectivity decreased slightly from 65.3 to 63.3 after the membrane was crosslinked with ethylene glycol [13], although the crosslinking mechanism is quite different from the thermal crosslinking considered here. Moreover, we anticipate that permeability and permselectivity may be enhanced even further once the membrane is pyrolyzed to a carbon molecular sieve (CMS) materials [36–38]. Pursuit of such carbon molecular sieve membranes is time consuming, but is under way and will be reported in a future paper.

Generally, when the permeability of a gas increases, the selectivity decreases. This behavior is easily understood: if the matrix is tightly packed, then the free volume or unoccupied space is reduced, thereby decreasing its ability to transport penetrants. Robeson reported an "upper bound" to the expected tradeoff relationship in 1991, and updated it in 2008 [5,6]. From Robeson's observations, regardless of the repeat unit, gas transport properties of solution-processable polymers do not exceed a certain boundary level, which is the upper limit of gas separation performance for current state of the art membranes.

The performances of 6FDA-based polyimides are compared to the "upper bound" trade-off lines in Fig. 5, in which all the polyimides exhibit excellent gas transport properties, lying near or above the so-called upper bound limits reported in 1991 and 2008, respectively. Consistent with the earlier discussion, for all gas pairs (He/O_2, He/N_2, He/CO_2, He/CH_4, O_2/N_2, N_2/CH_4, CO_2/N_2, CO_2/CH_4), 6FDA/DAM in Fig. 5 exhibits the highest permeability and lowest selectivity, while 6FDA-mPDA:DABA (3:2) has the highest selectivity and lowest permeability. The performance of other polyimides are between those of 6FDA/DAM and 6FDA-mPDA:DABA (3:2) polymers. The difference in both selectivity and permeability are larger when He is the faster permeating gas in the gas pairs, and the difference in selectivity is smaller for the gas pair of CO_2/N_2 and N_2/CH_4. Based on gases separation performance difference, the polyimides can be placed in two groups, one includes the 6FDA-mPDA, 6FDA-DABA, and 6FDA-mPDA:DABA (3:2) polymers (high selectivity and low permeability); the other includes 6FDA-DAM, 6FDA-DAM:DABA (3:2), and 6FDA-DAM:mPDA (3:2) polymers (low selectivity and high permeability). Obviously, DAM moieties contribute to high permeability in these latter polymers.

The above observations and upper bound correlations, however, do not address the key issue related to plasticization that is encountered in aggressive high CO_2 content feeds. As noted above, and discussed in more detail later in this paper, only the DABA-containing family materials are likely to be useful in this
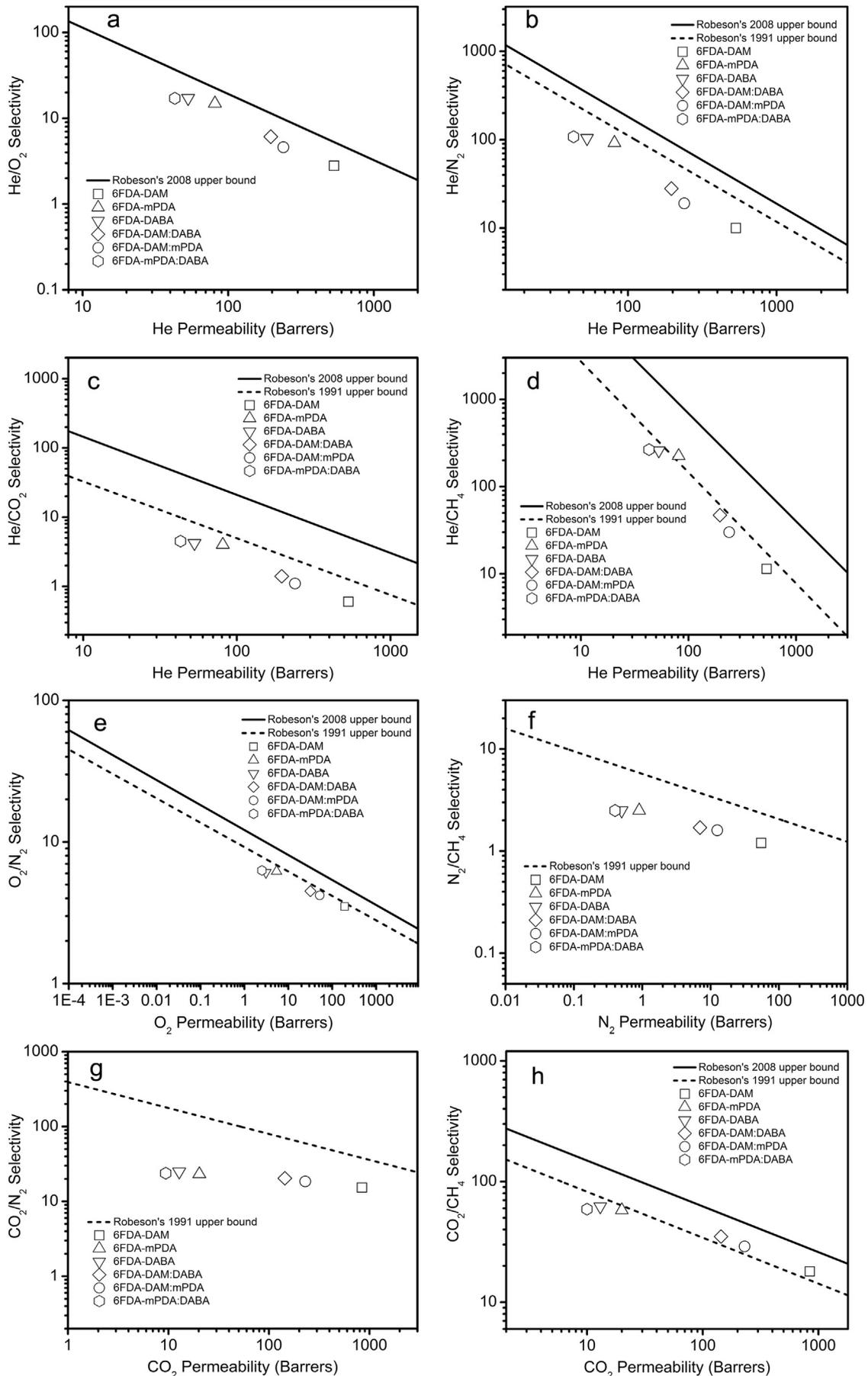
Fig. 5. Permeability−selectivity trade-off performance of 6FDA-based polyimides and comparison of the "Upper Bound".
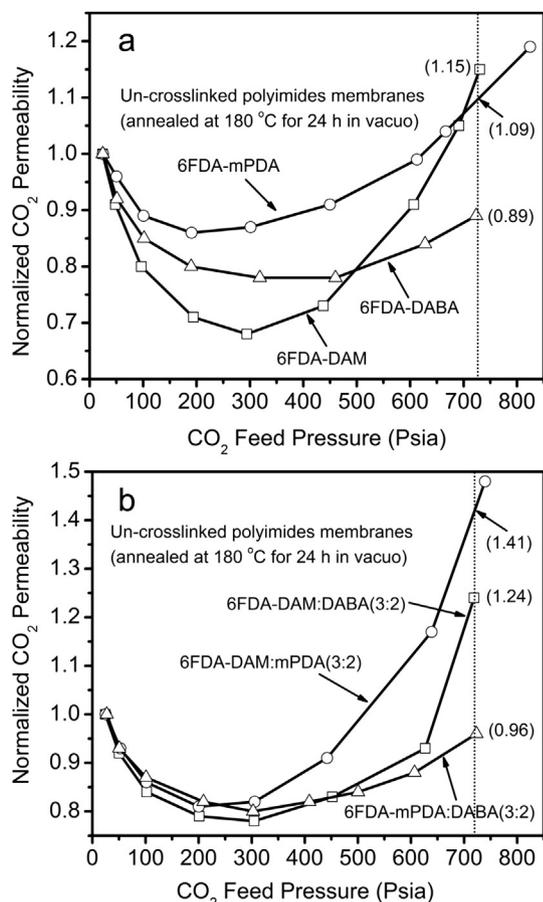
Fig. 6. Plasticization pressures vs. chemical structures of (a) homopolyimides, and (b) copolyimides. Feeds were all pure CO_2 at 35 °C.

important case. We probed the criticality of crosslinking as a means for suppressing plasticization. In this section, the very important plasticization response is correlated to the chemical structure of polyimides. To probe the importance of actual covalent crosslinking, all membranes were annealed at 180 °C for 24 h under vacuum and as noted earlier they remained un-crosslinked. The CO_2 plasticization pressures of the polyimides were evaluated by plotting the normalized permeability (equal to the permeability divided by the permeability at the initial feed pressure of 25 psia) vs. the CO_2 partial pressure in Fig. 6. This figure indicates that un-crosslinked 6FDA-mPDA (Fig. 6a) and 6FDA-DAM:mPDA (3:2) (Fig. 6b) samples show plasticization below 300 psia. On the other hand, 6FDA-DAM (Fig. 6a), 6FDA-DAM:DABA (3:2) (Fig. 6b), and 6FDA-mPDA:DABA (Fig. 6b) membranes show a plasticization pressure near 300 psia. Finally, the 6FDA-DABA membrane (Fig. 6a) shows the highest plasticization resistance response at about 450 psia. Although the plasticization degree of the polymers varied with feed pressures after plasticization, at the highest experimental pressure of about 720 psia, the normalized CO_2 permeability showed an order of severity of plasticization to be: 1.41 for 6FDA-DAM:mPDA (3:2) > 1.24 for 6FDA-DAM:DABA (3:2) > 1.15 for 6FDA-DAM > 1.09 for 6FDA-mPDA > 0.96 for 6FDA-mPDA:DABA (3:2) > 0.89 for 6FDA-DABA; this indicates that DAM-based polyimides were plasticized more seriously than the DABA-based polyimides. The hydrogen bonds between −COOH groups in DABA moieties yield polymers plasticization resistance. Despite this stabilization even for the DABA containing members of the family, in the absence of co-valent crosslinking, it is unlikely that adequate stability can be achieved for the most aggressive feeds.

4.3. Mixed gas permeation behaviors in polymers with related chemical structures

Mixed gas permeation behavior was also tested for two copolymers, un-crosslinkable 6FDA-DAM:mPDA (3:2) and 6FDA-DAM:DABA (3:2) which is, in principle, crosslinkable through DABA moieties. Permeation measurements were made with two feed mixtures of CO_2/CH_4 (10.3% and 50.0% CO_2 content) at 35 °C for up to 1000 psia feed pressure. A high retentate flow was used during these tests with a ratio of permeate/retentate flow less than 0.005 to minimize effects of concentration polarization. For all permeation experiments, the membrane was exposed to the feed for adequate time to reach steady state (typically at least 2 h) as indicated by the constant rate of pressure rise in the downstream reservoir. As the feed pressure increases, the gas phase components behave non-ideally; therefore, the fugacity coefficients of CO_2 and CH_4 were used to calculate the permeability coefficients.

Permeation results for mixed gas CO_2/CH_4 with a CO_2 mole content of 10% for 6FDA-DAM:mPDA (3:2) membrane are given in Fig. 7a and b. No plasticization was observed up to 1000 psia testing pressure, since the plasticization pressure for pure CO_2 was measured at about 200−300 psia. Indeed, the plasticization pressure is expected to be very high for actual mixed gas: about 2000−3000 psia for CO_2/CH_4 with 10% CO_2, and 400 to 600 psia for CO_2/CH_4 with 50% CO_2, since reduced fugacity coefficients for CO_2 may reduce the effective fugacity in comparison to simple partial pressure applicable at low total pressure [39]. The permeability of both CO_2 and CH_4 are close to the corresponding values from pure gas measurements at lower pressure as shown also in Fig. 3b and Table 2, while the separation factor is higher in mixed gas, presumably due to competitive dual-mode sorption effects [40,41]. The permeabilities of CO_2, CH_4, and the CO_2/CH_4 separation factor decrease with increasing of feed pressure, and finally reach a constant value at high feed pressure.

The mixed-gas permeability and separation factor for CO_2/CH_4 with a more aggressive feed of 50% CO_2 for a 6FDA-DAM:mPDA (3:2) membrane is shown in Fig. 7c and d. The behavior is clearly different from the case with 10% CO_2. The initial plasticization response was observed at about 300 psia, where both the CO_2 and CH_4 permeabilities increase and the CO_2/CH_4 decreases. At about 700 psia, more serious plasticization is apparent in Fig. 7d. Under the same CO_2 pressure, mixed gas measurements still shows a higher separation factor than the value from the pure gases measurement, again possibly due to successful competition of the CO_2 vs. CH_4 for sorption and transport sites in the glassy polymer.

Permeation results for mixed gas CO_2/CH_4 for 6FDA-DAM:DABA (3:2) membrane were reported earlier [17]. Similar to a 6FDA-DAM:mPDA (3:2) membrane, no plasticization was observed for mixed gas CO_2/CH_4 with a 10% CO_2, with the permeability of CO_2, CH_4, and CO_2/CH_4 separation factor also decreasing with increasing of feed pressure, and finally reaching a stable value. For mixed gas CO_2/CH_4 with 50% CO_2, CO_2 permeability shows a minimum value near 500 psia feed pressure, where a significant increase is seen for the permeability of CH_4, accompanied by a drop in separation factor, presumably indicating the onset of a plasticization response.

4.4. Crosslinking of polyimides for aggressive feed applications

Even without crosslinking, this family of materials shows very good resistance to the aggressive CO_2 feed conditions, especially to natural gas feed with lower CO_2 content such as 10% CO_2. On the other hand, at higher CO_2 concentrations, the tendency for plasticization in mixed gas measurements is of concern for such an aggressive feed. The crosslinking of membrane is absolutely necessary.
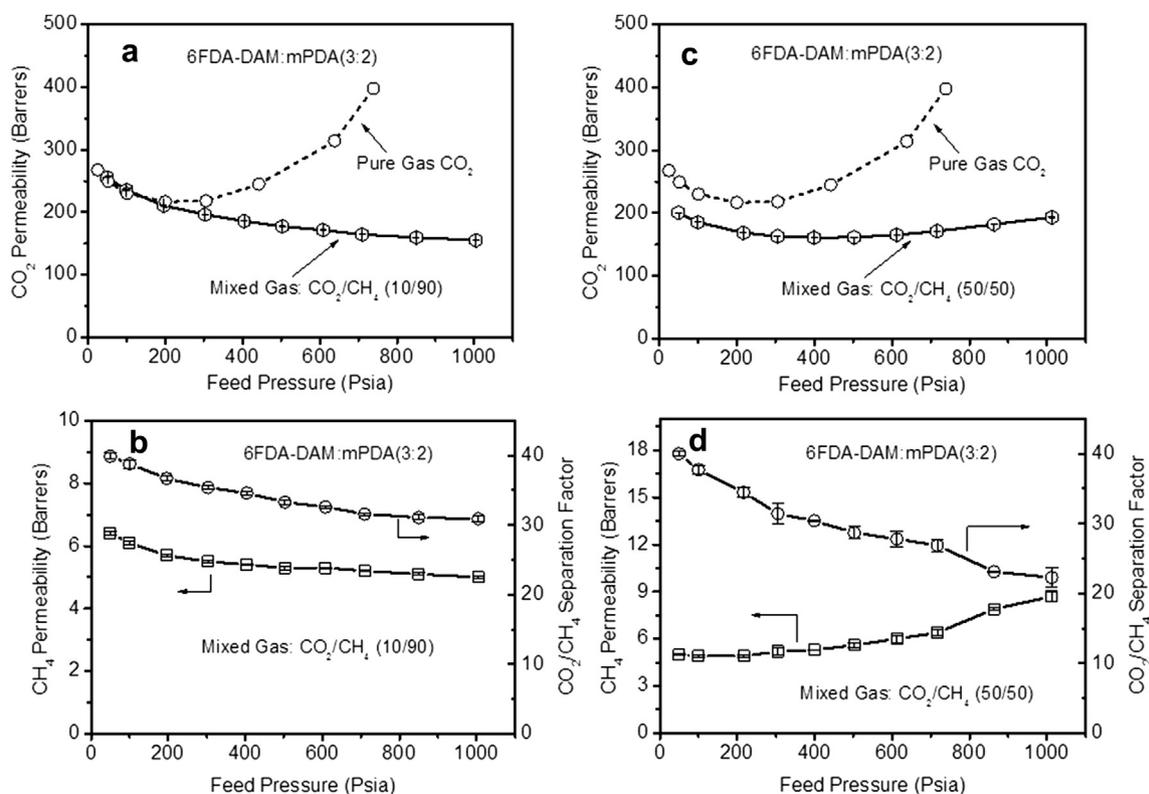
Fig. 7. Permeability and separation factor of 6FDA-DAM:mPDA (3:2) membranes for mixed gas (a) and (b) CO_2/CH_4 (10/90), (c) and (d) CO_2/CH_4 (50/50) at 35 °C. Pure gas CO_2 permeability is shown also for easy comparison.

The so-called ester-based crosslinking approach using propanediol, reported earlier for other DABA-containing polyimides [7,10,21,22,42], would also be applicable to the structures considered here. For instance, 6FDA-6FpDA:DABA (2:1) cross-linked with ethylene glycol prolonged the pure CO_2 plasticization pressure as indicated by the permeability which decreased with increasing of feed pressure up to 450 psia [21]. The performance of cross-linked 6FDA-DAM:DABA (2:1) membranes was found dependent on the crosslinking agent length, flexibility and the thermal treatment conditions [22]. Increased crosslinking temperatures for 1,3-propanediol crosslinking, 6FDA-DAM:DABA (3:2) showed higher CO_2 permeability with slightly increased selectivity [7]. Defect-free asymmetric hollow fiber were spun successfully and cross-linked with 1,3-propanediol, and were used for CO_2/CH_4 (20/80, 50/50) mixed gas separation. These cross-linked hollow fibers showed plasticization resistance. The foregoing results show that separation performance is influenced by many factors, including: the method for imidization, monoesterification process, crosslinking density, and fiber spinning [10,42].

Besides ester-crosslinking, thermally induced decarboxylation crosslinking of the 6FDA-DAM:DABA (3:2) membrane [8], especially the sub-T_g crosslinking [17] was shown to be an attractive alternate to the above ester crosslinking method. The decarboxylation induced crosslinking produced excellent plasticization resistance, which is apparent throughout the feed range of our equipment up to 700 psia for pure CO_2 gas or 1000 psia for 50% CO_2 mixed gas feed. The CO_2 permeability increased significantly, while the CO_2/CH_4 selectivity decreased moderately with increasing of crosslinking temperature [17]. Unlike the ester bond crosslinking sites which might have hydrolytic stability issue in acidic moisture, the thermal decarboxylation induced crosslinking sites are stable. As discussed earlier, 6FDA-mPDA:DABA (3:2) has higher intrinsic CO_2/CH_4 selectivity than 6FDA-DAM:DABA (3:2), and can be cross-

linked also through both ester-based crosslinking and decarboxylation-induced thermal crosslinking methods, depending on application demands. These properties make the 6FDA-mPDA:DABA (3:2) particularly attractive for the next generation of membranes in such aggressive feeds.

5. Conclusions

Six polyimides with related but significantly different chemical structures were synthesized, and their gas transport properties were evaluated particularly for their potential use in natural gas purification. Gas separation performance of the resulting membranes was correlated with the polyimide chemical structures. The results showed that both permeability and selectivity can be tailored through tuning of the packing density by adjusting monomer choice and composition. The CO_2 plasticization behavior of the membranes was also related to the polyimide structure; plasticization resistance can be enhanced through crosslinking of the polyimide through specific crosslinkable sites. These polyimides showed excellent performance among the polymeric membrane family, and most of these polyimides showed very good plasticization resistance under aggressive feed conditions. Future asymmetric hollow fiber formation and conversion to carbon molecular sieve membranes will be considered for these materials with the view towards large scale practical applications.

References

[1] Baker RW, Lokhandwala K. Ind Eng Chem Res 2008;47(7):2109–21.
[2] Datta AK, Sen PK. J Membr Sci 2006;283(1–2):291–300.
[3] Wind JD, Paul DR, Koros WJ. J Membr Sci 2004;228(2):227–36.
[4] Schell WJ. J Membr Sci 1985;22(2–3):217–24.
[5] Robeson LM. J Membr Sci 1991;62(2):165–85.
[6] Robeson LM. J Membr Sci 2008;320(1–2):390–400.
[7] Hillock AMW, Koros WJ. Macromolecules 2007;40(3):583–7.
[8] Kratochvil AM, Koros WJ. Macromolecules 2008;41(21):7920–7.
[9] Omole IC, Adams RT, Miller SJ, Koros WJ. Ind Eng Chem Res 2010;49(10): 4887–96.
[10] Omole IC, Miller SJ, Koros WJ. Macromolecules 2008;41(17):6367–75.
[11] Schmeling N, Konietzny R, Sieffert D, Rolling P, Staudt C. Beilstein J Org Chem 2010;6:789–800.
[12] Wieneke JU, Staudt C. Polym Degrad Stabil 2010;95(4):684–93.
[13] Staudt-Bickel C, Koros WJ. J Membr Sci 1999;155(1):145–54.
[14] Hillock AMW, Miller SJ, Koros WJ. J Membr Sci 2008;314(1–2):193–9.
[15] Horn NR, Paul DR. Polymer 2011;52(7):1619–27.
[16] Qiu WL, Chen CC, Kincer MR, Koros WJ. Polymer 2011;52(18):4073–82.
[17] Qiu WL, Chen CC, Xu LR, Cui LL, Paul DR, Koros WJ. Macromolecules 2011;44(15):6046–56.
[18] Neyertz S, Brown D, Pandiyan S, van der Vegt NFA. Macromolecules 2010;43(18):7813–27.
[19] Staudt-Bickel C. Soft Mater 2003;1(3):277–93.
[20] Rolling P, Lamers M, Staudt C. J Membr Sci 2010;362(1–2):154–63.
[21] Wind JD, Staudt-Bickel C, Paul DR, Koros WJ. Ind Eng Chem Res 2002;41(24): 6139–48.
[22] Wind JD, Staudt-Bickel C, Paul DR, Koros WJ. Macromolecules 2003;36(6): 1882–8.
[23] Chen CC, Qiu WL, Miller SJ, Koros WJ. J Membr Sci 2011;382(1–2):212–21.
[24] Stern SA, Mi Y, Yamamoto H, Stclair AK. J Polym Sci Pol Phys 1989;27(9): 1887–909.
[25] Yamamoto H, Mi Y, Stern SA, Stclair AK. J Polym Sci Pol Phys 1990;28(12): 2291–304.
[26] Matsumoto K, Xu P. J Membr Sci 1993;81(1–2):23–30.
[27] Stern SA, Liu Y, Feld WA. J Polym Sci Pol Phys 1993;31(8):939–51.
[28] Tanaka K, Osada Y, Kita H, Okamoto KI. J Polym Sci Pol Phys 1995;33(13): 1907–15.
[29] Shimazu A, Miyazaki T, Maeda M, Ikeda K. J Polym Sci Pol Phys 2000;38(19): 2525–36.
[30] Guzman-Gutierrez MT, Rios-Dominguez MH, Ruiz-Trevino FA, Zolotukhin MG, Balmaseda J, Fritsch D, et al. J Membr Sci 2011;385(1–2):277–84.
[31] Prausnitz JM, Lichtenthaler RN, Azevedo EGd. Molecular thermodynamics of fluid-phase equilibria. 3rd ed. Upper Saddle River, N.J.: Prentice Hall PTR; 1999.
[32] CRC handbook of chemistry and physics. Boca Raton, FL: Chapman and Hall/ CRCnetBASE; 1999.
[33] Wind JD. Improving polyimide membrane resistance to carbon dioxide plasticization in natural gas separations. Ph.D. thesis. The University of Texas at Austin; 2002.
[34] Barsema JN, Klijnstra SD, Balster JH, van der Vegt NFA, Koops GH, Wessling M. J Membr Sci 2004;238(1–2):93–102.
[35] Zhao HY, Cao YM, Ding XL, Zhou MQ, Liu JH, Yuan Q. J Membr Sci 2008;320(1– 2):179–84.
[36] Rungta M, Xu LR, Koros WJ. Carbon 2012;50(4):1488–502.
[37] Xu LR, Rungta M, Koros WJ. J Membr Sci 2011;380(1–2):138–47.
[38] Kiyono M, Williams PJ, Koros WJ. Carbon 2010;48(15):4432–41.
[39] Omole IC. Crosslinked polyimide hollow fiber membranes for aggressive natural gas feed streams. Georgia Institute of Technology, Ph.D. thesis. Georgia Institute of Technology; 2008.
[40] Tshudy JA, Frankenb CV. J Polym Sci Pol Phys 1973;11(10):2027–37.
[41] Michaels AS, Barrie JA, Vieth WR. J Appl Phys 1963;34(1):1–12.
[42] Ma CH, Koros WJ. J Membr Sci 2013;428:251–9.